THE WAVEFIELD OF AN ULTRASONIC ANGLE BEAM SHEAR WAVE TRANSDUCER: AN ELASTODYNAMIC APPROACH

Terence P. Lerch and Lester W. Schmerr
Center for NDE and the Department of Aerospace Engineering and Engineering Mechanics
Iowa State University
Ames, Ia 50011

Alexander Sedov
Department of Mechanical Engineering
Lakehead University
Thunder Bay, Ontario
Canada P7B 5E1

INTRODUCTION

Inspection of welded plate and pipe assemblies with ultrasonic angle beam shear wave transducers is an important and common application of ultrasonic NDE. With the advent of the Thompson and Gray measurement model [1], many practical ultrasonic testing configurations such as angle beam inspections can now be analytically modeled. An important component of the measurement model for any UT testing configuration is the calculation of the incident wavefields radiated by the transmitting transducer, commonly known as the transducer beam model.

Many previous studies of angle beam shear wave transducers have concentrated on detection methods for particular types of defects in the welds such as cracks, inclusions, slag, etc., and have treated the transducer beam model as an afterthought. Little effort was spent on modeling the angle beam transducer itself. Over the past few years, we have turned our attention specifically to the incident wavefields produced by these transducers and investigated a number of beam models that can be applied to these types of inspection problems. Comparisons of models based on Gauss-Hermite expansions, boundary diffraction waves, paraxial and non paraxial approximations have been made [2,3] for unfocused transducers residing in a fluid and oriented obliquely incident to planar fluid-solid interfaces (see Figure 1a). In these models, the first medium was taken to be a fluid, while in reality, angle beam transducers actually employ a contact compressional wave transducer acting on the surface of an elastic solid wedge. While it seems likely one could neglect the shear properties of the wedge since the contact transducer primarily generates P-waves in the wedge, no one to our knowledge has rigorously examined this assumption. By developing a more complete elastodynamic (solid-solid) transducer beam model which includes all the possible bulk wave modes in both the transducer wedge and the interrogated material, we can examine this assumption and compare the results of this latest model with previous ones that have replaced the wedge material with an equivalent fluid.

Review of Progress in Quantitative Nondestructive Evaluation, Vol. 16
Edited by D.O. Thompson and D.E. Chimenti, Plenum Press, New York, 1997

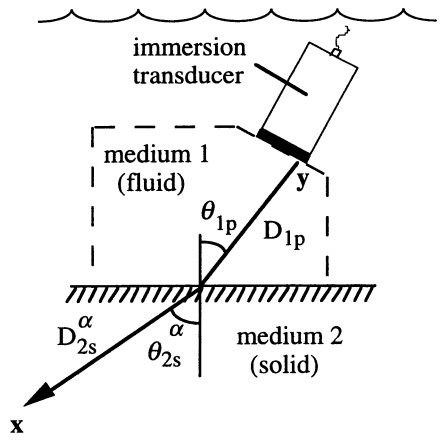

Figure 1a. An unfocused transducer radiating through a planar fluid-solid interface oriented at oblique incidence.

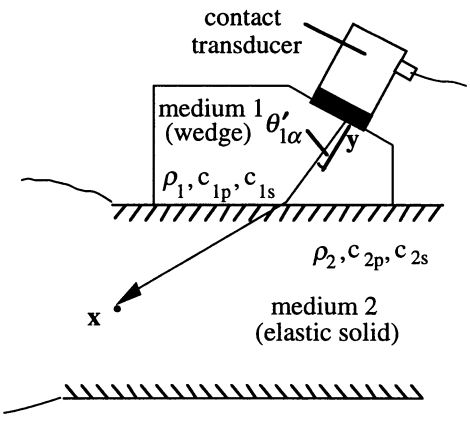

Figure 1b. An angle beam shear wave transducer interrogating an elastic solid (welded plate)

The incident wavefields transmitted into a material being inspected by an angle beam shear wave transducer can be modeled in a two step process, as discussed in [2,3]. First, the wavefields in the wedge material of the transducer are determined by modeling the angle beam probe as a planar, contact transducer radiating into an isotropic, homogeneous, elastic half-space, which results in an expression for the incident displacements in the wedge that is very similar to the Rayleigh-Sommerfeld integral. Second, the first medium (wedge) wavefields will be transmitted through the planar interface between the transducer wedge and the material being interrogated and into the interior of the second isotropic, homogeneous, elastic medium, ultimately leading to the final form of the elastodynamic model for this particular type of transducer.

As the basis for this model, we'll start with the angular plane wave spectrum approach of Vezzetti [4]. Plane wave representations of the solution for the elastic wave equation are convenient since they allow us to properly incorporate the boundary conditions, both at the contact transducer-wedge interface, and the wedge-underlying material interface (see Figure 1). These angular spectrum integrals are evaluated by the method of stationary phase and lead to expressions similar in form to the Rayleigh-Sommerfeld surface integral for a piston transducer in a fluid. These surface integrals can be evaluated numerically by using edge elements, as discussed in [3]. Comparisons of this latest model with the more approximate models assuming an equivalent fluid-like material for the transducer wedge will be made later in the paper. Because of the extensive nature of the model derivation and the limited amount of space currently available, only the resulting expression will be shown here.

CONTACT TRANSDUCER ON AN ELASTIC SOLID

Before considering the incident displacement wavefields in the second medium (material of interrogation), we must first model the wavefields in the first medium (transducer wedge) in order to determine the directivity amplitude functions characteristic of the first medium. The contact transducer will be modeled as a distributed stress source acting on the plane surface of an elastic half-space, i.e. the transducer wedge. As Vezzetti did [4], we will also represent the wavefield in the wedge as an angular spectrum superposition of three sets of plane waves, where one set is composed of purely compressional waves, and the remaining two are purely orthogonal, transverse waves.

The boundary conditions along the compressional contact transducer and the wedge interface must be declared before evaluation of the angular spectrum of plane waves can

begin. For this particular interface, we assume the circular compressional wave transducer imparts a uniform pressure, p_0, to the elastic solid half-space (wedge) only over the active area of the transducer surface, with no other sources existing on the wedge. We will also assume the shearing stresses at this interface will vanish. Once these boundary conditions are implemented, and a considerable amount of algebraic simplification is made, the method of stationary phase (see Stamnes [5,6]) can be utilized to explicitly evaluate the angular plane wave spectra and obtain more physically relevant expressions for the displacement fields.

After the method of stationary phase is applied and more algebraic simplification done, we arrive at an expression for the incident displacement wave fields in the first medium material that is composed of two terms, where each term is similar in form to the Rayleigh-Sommerfeld integral. In other words, for each term (one representing compressive waves, the other representing shear waves), we have a superposition of spherical waves being summed over the active area of the transducer face. However, in this elastodynamic model, these spherical wave sources are modified by directivity functions, $K_p(\theta'_{1p})$, $K_s(\theta'_{1s})$, and polarization vectors, $\mathbf{d}^P$ and $\mathbf{d}^S$, for the compressive and shear wave terms, respectively. The compressive and shear wave directivity functions are explicitly stated in [7], and depend only on the wedge material's wavespeeds, c_{1p}, c_{1s}, and the incident angles, θ'_{1p}, θ'_{1s} for the compressive and transverse waves, respectively. The angles θ'_{1p} and θ'_{1s} are measured between the propagation vectors for each type of wave and the normal to the wedge surface, as shown in Figure 1b. These directivity functions, which are a by-product of the boundary conditions imposed on the contact transducer-wedge interface, will carry over to the complete angle beam model and directly affect the incident wavefields predicted in the second medium. When the wavespeeds are fixed and the directivity function values are computed as a function of their respective incident angles, θ'_{1p}, θ'_{1s}, we find that $K_P(\theta'_{1p}) \cong 1$ and $K_s(\theta'_{1s}) \cong 0$ for small incident angles. This observation becomes very important when the complete elastodynamic model is used to calculate incident displacement fields in the second medium.

ANGLE BEAM TRANSDUCER MODEL

Since the main objective of analytically modeling an angle beam shear wave transducer is to derive the expression for the incident displacement fields in the material of interrogation (second medium), the first medium wavefield results must be extended across the planar interface between the first and second media (wedge-elastic solid). The boundary conditions assumed at this particular interface (as opposed to the earlier contact transducer-wedge interface) will play an important and unique role in the transmission process of both the compressive and shear wave fields. Both the sets of incident P and S waves will be transmitted from the transducer wedge into the second medium. Through this transmission process, the two incident waves will each refract into a pair of transmitted P waves and S waves, making a total of four distinct bulk waves in the solid being inspected. The relative contribution of each of these bulk waves can then calculated, with special attention paid to the contributions coming from the incident shear wave, since these are the waves neglected by the majority of previous angle beam transducer models.

The additional effects of the planar interface between the wedge and elastic solid on the elastodynamic model must be discussed. A thin layer of fluid couplant is typically used in practice to improve the transmission of energy from the transducer wedge to the material under interrogation. While the wavefields within the couplant itself will not be modeled, the effects of the couplant on the transmission process will be included by considering the two elastic solids to be in smooth contact. The continuity of normal stresses and displacements across the interface is conserved, but the shear stresses at the interface are assumed to be zero. These boundary conditions result in plane wave transmission coefficients, $T_{12}^{\alpha,\beta}$, for each of the four bulk waves, where the α; β superscript represents a transmitted wave of type α $(\alpha=P,SV)$, due to an incident wave of type β $(\beta=P,SV)$.

Explicit expressions for these transmission coefficients are given in [7]. The planar interface also allows the total incident shear wave in the first medium to be decomposed into two orthogonal parts, SV and SH. Recall that the SH portion of the shear wave will not propagate through the interface because of the fluid couplant. Note also that only a fraction of the SV wave will be transmitted, i.e., the component of the SV wave traveling in the incident shear wave direction, $(\mathbf{d}^S \cdot \mathbf{e}_{SV})$, where $\mathbf{d}^S$ is the polarization unit vector of the shear waves and $\mathbf{e}_{SV}$ is the propagation unit vector of the SV component of the shear waves.

We return to Vezzetti and his plane wave expansion representation of the incident P and S wavefields in the first medium. With our arbitrary field point of interest ($\mathbf{x}$ in Figure 1) now located in the second medium, certain modifications must be made to the angular plane wave expansion terms originating in the first medium. These modifications include multiplying the plane wave amplitudes by the appropriate transmission coefficients, correcting the orientation of the polarization unit vectors as they refract into the second medium, and changing the plane wave phase terms to account for the field point, $\mathbf{x}$, now being in the underlying solid. With these modifications made to the angular spectrum of plane waves, the method of stationary phase once again can be implemented to express the wavefields of this elastodynamic model in terms of physical quantities, which results in four terms (one for each wave type), with each term resembling the Rayleigh-Sommerfeld integral. However, because of the transmission through the planar interface, the spherical waves characteristic of the Rayleigh-Sommerfeld integral now become elliptical waves that are modified by transmission coefficients, directivity functions, and polarization unit vectors. At this point, the incident wavefields of the elastodynamic model could be evaluated through direct numerical integration procedures, but this type of evaluation would be computationally costly to do because of the two dimensional nature of the integration. By using the edge element technique discussed in earlier papers [3,7], the post stationary phase form of the wavefields can be significantly simplified (numerically) by reducing the order of integration from 2-D to 1-D, thus saving computational time while retaining the same level of accuracy as the more numerically intensive approaches. A paraxial assumption could also be made at this juncture [2], but in this case, a certain amount of accuracy would be lost in the very nearfield areas of the wavefield.

When the edge element technique is implemented, the incident displacement wavefields in the second medium for this solid-solid planar interface model can be expressed as:

$$\mathbf{u}(\mathbf{x},\omega) = \frac{p_0}{2\pi(\rho_1 c_{1p}^2)} \sum_{\alpha=P,S} \left\{ \sum_{m=1}^{M} \sum_{c=1}^{C} \frac{(T_{12}^{\alpha,P})^m K_p([\theta_1'^{\alpha,P}]^m)\mathbf{d}_m^{\alpha,P} \exp[i\phi_m^{\alpha,P}]}{[(\Delta_{x0}^{\alpha P})^m(\Delta_{y0}^{\alpha P})^m]^{1/2}} I_{mc}^{\alpha,P} \right\} +$$

$$\frac{p_0}{2\pi(\rho_1 c_{1s}^2)} \sum_{\alpha=P,S} \left\{ \sum_{m=1}^{M} \sum_{c=1}^{C} \frac{(T_{12}^{\alpha,SV})^m K_s([\theta_1'^{\alpha,SV}]^m)(\mathbf{d}^{1s} \cdot \mathbf{e}_{SV})_m^{\alpha} \mathbf{d}_m^{\alpha,SV} \exp[i\phi_m^{\alpha,SV}]}{[(\Delta_{x0}^{\alpha SV})^m(\Delta_{y0}^{\alpha SV})^m]^{1/2}} I_{mc}^{\alpha,SV} \right\} \tag{1}$$

where the first term corresponds to the contribution coming from the incident P-waves in the first medium, and the second term corresponds to the incident SV-waves in the first medium. Each finite summation on m represents the discretization of the transducer surface into planar area elements (typically triangles or quadrilaterals). The finite summation on c represents the straight contour edges that bound each of the area elements. Both of these summations (m,c) are a consequence of applying the edge element method to simplify the numerical evaluation of the Rayleigh-Sommerfeld-like form of the elastodynamic model. In a general sense, it is the individual contribution of each of these edge elements, c, that is summed for each area element, m, (for each of the four bulk waves) that gives the incident displacement wavefields in the second medium.

Qualitatively, each of the terms in Eqn. (1) are listed below. As mentioned earlier, the $\alpha;\beta$ superscripts correspond to a refracted wave of type α $(\alpha=P,SV)$ due to an incident wave of type β $(\beta=P,SV)$.

$\phi_m^{\alpha,\beta}$ - the phase argument for the mth area element of the discretized transducer surface

$I_{mc}^{\alpha,\beta}$ - the edge element contribution made by the cth edge of the mth area element of the discretized transducer surface

$\mathbf{d}^{\alpha,\beta}$ - the polarization unit vectors for the mth area element of the discretized transducer surface

$(\mathbf{d}^{1s}\cdot\mathbf{e}_{SV})^{\alpha}$ - the component of the incident SV-wave that transmits through the interface and into the second medium

$\Delta_x^{\alpha,\beta}$, $\Delta_y^{\alpha,\beta}$ - the geometrical spreading terms (elliptical in nature) presented in previous works [2,3,7]

As was shown in [7], edge elements can also be applied to this fluid-solid planar interface problem, where the incident displacements in the second medium are

$$\mathbf{u}(\mathbf{x},\omega) = \sum_{\alpha=P,S} \frac{-\rho_1 c_{1p} v_0}{2\pi i \omega \rho_2 c_{2\alpha}} \sum_{m=1}^{M}\sum_{c=1}^{C} \frac{(T_{12}^{\alpha,P})^m \mathbf{d}_m^{\alpha,P} \exp[i\phi_m^{\alpha,P}]}{[(\Delta_{x0}^{\alpha P})^m (\Delta_{y0}^{\alpha P})^m]^{1/2}} I_{mc}^{\alpha,P} \qquad (2)$$

Note that the only difference between the fluid-solid interface model shown above and the incident P-wave contributions of the solid-solid interface model is the directivity function, $K_p(\theta'_{1p})$, in the solid-solid model. In the model comparisons section, we will briefly compare the incident P-wave components of both models and examine the effect of the directivity function in the elastodynamic (solid-solid interface) model.

COMPARISONS

Both the fluid-solid and solid-solid interface models have the ability to compute entire refracted longitudinal wave fields and mode converted shear wave fields over the full range of possible refracted angles (that produce bulk waves) in the second medium due to an incident longitudinal wave in the first medium. As mentioned earlier, since the transducer wedge material is being modeled as an elastic solid in the solid-solid interface model, it is also capable of computing the additional transmitted wave contributions due to the incident S-waves in the wedge material as well. The wavefields consist of complex displacement values (calculated in the frequency domain) with both amplitude and phase components, where the polarization vectors determine the orientation of the displacement amplitudes. The models are general enough to allow the user to choose the size, type, position, and orientation of the transducer with respect to the planar interface, and the material properties of the two media. The model expressions are evaluated at a fixed, single frequency, which, in this paper, is taken as the center frequency of the transducer.

We will restrict our comparisons to central axis, linear scan profiles where the profile is computed along the refracted central axis of the transducer in the second medium and is essentially equivalent to an on-axis profile in a one medium problem (see Figure 3). The profiles consist of the absolute magnitudes of the incident displacements calculated at individual field points along these lines. Two types of comparisons will be made: 1) all four wave contributions of the solid-solid interface model will be displayed and compared at a refracted angle of 45° (based on the mode refracted SV wave resulting from an incident

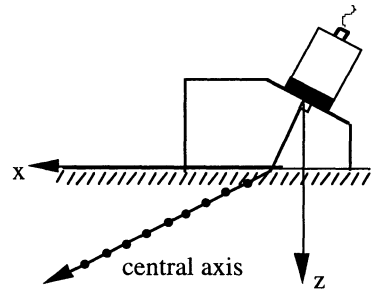

Figure 3. Schematic of the central axis profile.

P wave), and 2) the mode converted shear wave profile refracted at an angle of 75° from an incident P-wave as computed by both the fluid-solid and solid-solid interface models. Lucite and steel, with their respective wavespeeds and impedances, were chosen as the two media to model in both the fluid-solid and solid-solid interface model expressions. Note that the z-axes plotted in the central axis comparisons correspond to a depth normal to the lucite-steel interface, and not the distances along the refracted ray (see Figure 3). An unfocused, 5MHz, 1/2 inch diameter transducer is modeled in both cases. The height of the lucite wedge measured from the center of the piezoelectric source was taken to be 1.8 cm, which is a common wedge distance found in commercially available probes. In both comparisons, the absolute magnitude of the 5 MHz frequency component is displayed, which is computed from the contour contributions of 2048 (32 radial x 64 angular) area elements associated with the edge element technique.

In Figure 4, the four wave types computed for a refracted axis of 45° are shown. It should be noted that since all four wave contributions (P-P, P-SV, SV-P, SV-SV) were computed along the central axis field points corresponding the P-SV wave, different path lengths and angles of incidence and refraction are expected for each wave type at each field point evaluated. As seen in Figure 4, the P-SV contribution makes by far the greatest contribution to the total displacement field, with the P-P, SV-P, and SV-SV wave types being essentially insignificant throughout the entire profile. This behavior is characteristic of similar comparisons made at higher refracted angles. At lower angles of refraction, the wave contributions resulting from the incident SV wave continued to be negligible. A brief explanation of this observed behavior will be discussed in the Conclusions section.

Figure 5 displays the P-SV wave contributions predicted by both the fluid-solid interface and elastodynamic models at an extreme refracted angle of 75°. No difference in amplitude can be visually detected between the two models. Again, similar behavior was observed at smaller angles of refraction, leading us to conclude that, for typical situations such as this, the P-wave directivity function has no significant effect on the transmitted wavefields coming from the incident P-waves in the lucite.

CONCLUSIONS

Based on the comparisons made among the different wave types for the lucite-steel planar interface, two general conclusions can be stated. First, of the four refracted wave types, the P-SV wave by far makes the most significant contribution to the total incident wave field in the second medium, even at rather slight angles of refraction. Although not shown here, we have observed that the P-P wave is only important at refracted angles of 30° or less, and both the SV-P and SV-SV waves are negligible at all angles of refraction. Second, the common practice of representing the first medium solid as an acoustic, or "fluid-like" medium, which propagates only longitudinal waves and no shear waves, does not compromise the overall accuracy of the total incident wave field found in the second medium for the particular solids modeled here. The insignificant magnitudes of the incident S-wave contributions, and the excellent correspondence between the fluid-solid and solid-

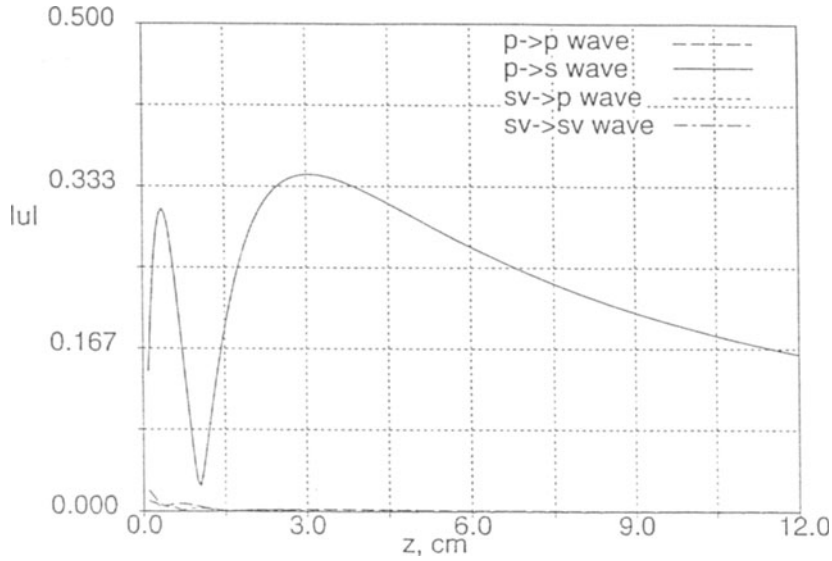

Figure 4. The normalized displacements of the four wave types predicted by the elastodynamic (solid-solid interface) model at a refracted angle of 45°.

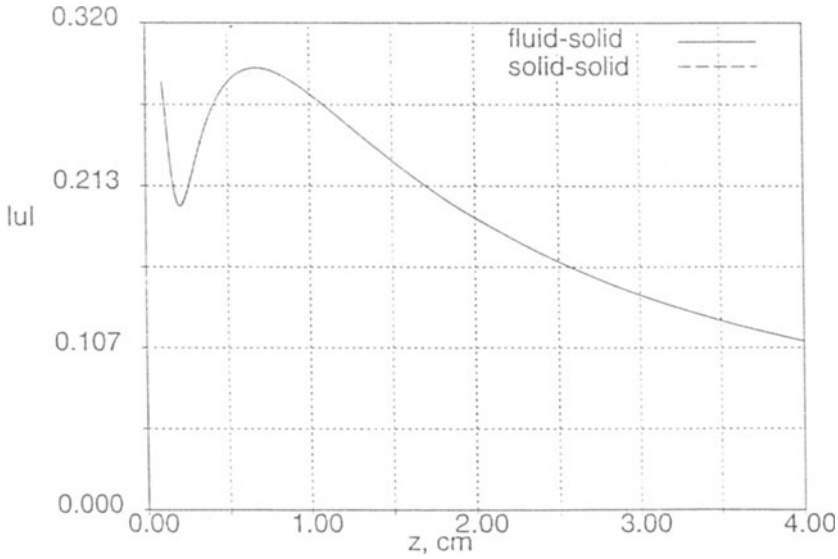

Figure 5. The P-SV wave central axis profiles predicted by the fluid-solid and solid-solid models at a refracted angle of 75°.

solid interface models shown in Figure 5, demonstrate the lack of influence of the S-waves in the transducer's wedge have on the transmitted displacement fields in the material of interrogation.

Both of these conclusions can be directly related to the behavior of the P-wave and S-wave directivity functions. When the incident angle ($\theta'_{1\alpha}$) on which these functions depend is small, the P-wave directivity function tends towards unity, while the S-wave function approaches zero. In all of the comparisons studied (of which we show only a small subset here), this critically important incident angle remained small. Thus, very little difference could be detected between the fluid-solid interface model and the elastodynamic model wave field comparisons, while the contributions coming from the incident SV waves are essentially nonexistent in the underlying elastic solid.

ACKNOWLEDGMENTS

L. Schmerr and T. Lerch were supported in this work by the Center for NDE, at Iowa State University. A. Sedov was supported by the Natural Sciences and Engineering Research Council of Canada.

REFERENCES

1. Thompson, R.B. and T.A. Gray, "A Model Relating Ultrasonic Scattering Measurements Through Liquid-Solid Interfaces to Unbounded Medium Scattering Amplitudes", J. Acoust. Soc. Am., 74, 1279-1290, 1983.
2. Lerch, T.P., Schmerr, L.W. and A. Sedov, "The Paraxial Approximation for Radiation of a Planar Ultrasonic Transducer at Oblique Incidence Through an Interface", *Review of Progress in QNDE,* D.O. Thompson and D.E. Chimenti, Eds., Plenum Press, N.Y., 14A, 1067-74, 1995.
3. Lerch, T.P., Schmerr, L.W. and A. Sedov, "Modeling the ultrasonic radiation of shear wave angle beam transducers", *Review of Progress in QNDE,* D.O. Thompson and D.E. Chimenti, Eds., Plenum Press, N.Y., 15A, 1011-1018, 1996.
4. D.J. Vezzetti, "Propagation of bounded ultrasonic beams in anisotropic media," *J. Acoust. Soc. Am.*, 78 (3), 1103-8, 1985.
5. J.J. Stamnes, *Waves in Focal Regions*, Adam Hilger, Boston, MA, 1986.
6. J.J. Stamnes, "Focusing of two-dimensional waves," J. Opt. Soc. Am., 71(1), 15-31, 1981.
7. T. P. Lerch, "Ultrasonic transducer characterization and transducer beam modeling for applications in nondestructive evaluation", Ph.D. Dissertation, Iowa State University, 1996.